

Extreme multiphoton coupling in molecular systems

George N. Gibson

Department of Physics, University of Connecticut, Storrs, Connecticut 06269

(Received 11 December 2002; published 3 April 2003)

Compared to single-photon rates, multiphoton excitation rates of atoms and molecules are generally quite small, even at high laser intensities, at least in a 2-level system. Small multiphoton coupling strengths, large ac Stark shifts, and ionization all inhibit real population transfer between bound states. However, it has recently been shown that a 3-level system consisting of a ground state and a pair of nearly degenerate strongly coupled upper states greatly enhances the multiphoton coupling with the ground state, while also greatly reducing the ac Stark shift of the ground state. In this paper I will derive an analytic expression for the n -photon Rabi frequency, for this system, in the case of degenerate upper states, as well as an expression for the level shifts induced in the case of nondegenerate upper states. Numerical calculations based on the 3-level system are presented to verify the analytic results and to show that high-order π pulses can be driven at moderate field strengths. To demonstrate the feasibility of this process in a real physical system, I will present fully correlated 2-electron calculations in a model one-dimensional molecular potential, including ionization that show a 12-photon π pulse driven with near-infrared photons. In other words, a single excited state 18.6 eV above the ground state can be populated with over 90% efficiency with little ionization while the ground state is almost completely depopulated. Besides the possibility of producing an amplifying medium in the vacuum ultraviolet, this 3-level configuration may open the door to other strong field effects previously restricted to single-photon interactions, such as adiabatic passage and inner-shell ionization.

DOI: 10.1103/PhysRevA.67.043401

PACS number(s): 33.80.Rv, 32.80.Rm, 42.50.Hz

I. INTRODUCTION

Multiphoton excitation with strong laser fields has been considered as a way of populating highly excited states of atoms and molecules with optical photons, perhaps to produce population inversions in the vacuum ultraviolet (VUV) [1,2]. Unfortunately, it has been shown that, within a 2-level model, multiphoton excitation rates are exceedingly small and that ionization will generally dominate the interaction [3]. The main problem is that the high laser intensities required to overcome the weak multiphoton coupling strength also produce large ac Stark shifts. These Stark shifts move the energy levels of the material in a complex way making it impossible to maintain a multiphoton resonance for an appreciable time during the laser pulse. Thus, the prospects for using strong laser fields for the excitation and control of real population did not appear to be promising.

More recently, a 3-level system has been proposed that provides a strong multiphoton coupling between the ground state and highly excited upper states, while, at the same time, minimizing the ac Stark shift of the ground state that would normally destroy the resonance between the laser field and the transition being driven [4]. The 3-level system consists of a ground state and a pair of nearly degenerate strongly coupled upper states. Under these conditions, multiphoton excitation is so strong that high-order π pulses can be considered, for the first time.

Not only does this model 3-level system work exceptionally well, all evenly charged homonuclear diatomic molecular ions have this level structure, where the upper states consist of the charge transfer states [5]. Indeed, for many years, this molecular configuration has been the one outstanding example of efficient multiphoton excitation [6–9], although there had been no explanation for this strong excitation until now.

This paper is divided into two main parts. In the first part, I will derive two important results for the 3-level system: an analytic expression for the n -photon Rabi frequency in the case of degenerate upper levels and a perturbative expression for the shifts for the upper states when they are nondegenerate. The two results allow one to predict the field strength and laser frequency needed to produce a multiphoton π pulse under a wide variety of conditions. In the second part, I will present fully correlated 2-electron calculations in a one-dimensional (1D) model molecular potential that includes ionization. These calculations are used to verify the analytic results and demonstrate that a single state 18.6 eV above the ground state can be populated through a 12-photon transition with high efficiency (>90%) and little ionization while completely depopulating the ground state.

Although efficient multiphoton excitation is itself significant, the interest here is in π pulses, for two reasons. First, π pulses produce the maximum possible inversion on a transition, which is important for optical gain. Second, adiabatic passage is a more robust means for population transfer. However, the ability to generate a π pulse is a prerequisite for adiabatic passage, where at least several Rabi oscillations are needed. As it turns out, the transition from producing a π pulse to achieving adiabatic passage is easier for a multiphoton transition than for a single-photon transition, although this will be the subject of another paper. This system may also show strong harmonic generation, but, this too will be the subject of another paper.

II. 3-LEVEL MODEL**A. Analytic solution of the degenerate 3-level model**

The 3-level system of interest is shown in Fig. 1 and can be represented by the following time dependent Hamiltonian:

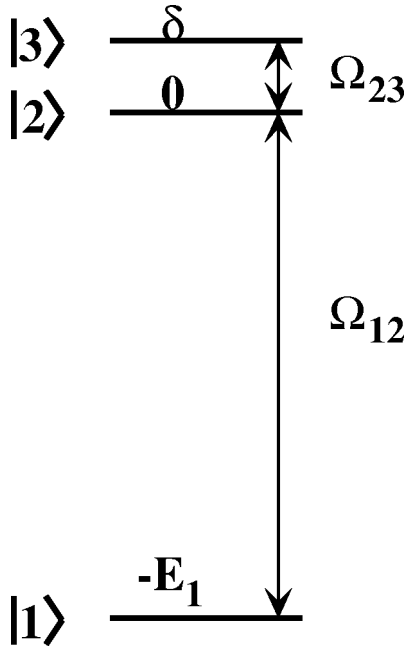


FIG. 1. The 3-level system showing the energies of the levels and the couplings between them.

$$H(t) = \begin{bmatrix} -E_1 & \Omega_{12}(t) & 0 \\ \Omega_{12}(t) & 0 & \Omega_{23}(t) \\ 0 & \Omega_{23}(t) & \delta \end{bmatrix}, \quad (1)$$

where $-E_1$ is the energy of level 1 ($E_1 > 0$), δ is the splitting of the upper states, and $\Omega_{ij}(t) = R_{ij} F_o f(t) \sin(\omega t)$. R_{12} and R_{23} are the dipole matrix elements between levels 1 and 2 and levels 2 and 3, respectively. F_o is the peak field strength, $f(t)$ is a normalized pulse envelope, and ω is the laser frequency. All quantities are in atomic units throughout this article. Since levels 2 and 3 are interchangeable, it does not matter which is coupled to level 1. For the purposes here, we are interested in the regime where $R_{23} \gg R_{12}$ and $E_1 \gg \omega$, although this is not a requirement of the derivation.

Before solving the 3-level system, it is worth making a comment on the choice of gauge for the interaction. Equation (1) explicitly uses the length form of the interaction. For numerical calculations on a grid, as will be presented in the following section, the results should be independent of the choice of the gauge, as long as the grid is large enough and fine enough. I have performed some checks comparing the length form Fx to the momentum form Ap , where A is the vector potential. Indeed, the results agree quite satisfactorily, demonstrating the independence on the gauge. Thus, the question of gauge only arises in an approximate model of the physical situation, such as the 3-level reduction analyzed here. The problem is that in the momentum form, the interaction between the upper states in this 3-level model is identically zero, because the states are assumed to be degenerate, and we have the relationship that $p_{23} = (im/\hbar)(E_2 - E_3)R_{23} = 0$ for $E_3 = E_2$ [10], where p_{23} is the momentum matrix element between states 2 and 3. Thus, the interaction between degenerate levels is extremely sensitive to the choice

of gauge. However, this issue has been thoroughly discussed in the context of the 2-photon transition from the $1s$ state to the $2s$ in hydrogen [10]. In this instance, if only the $1s$, $2s$, and $2p$ states are included in the calculation, the 2-photon rate is within 50% of the actual value using the length gauge, while the velocity gauge gives zero, due to the degeneracy between the $2s$ and $2p$ states. Thus, for levels with small energy differences, the length gauge will be much more accurate and is the clear choice.

In this section, I will consider just the case of degenerate upper levels ($\delta = 0$). Under this condition, if the amplitudes of the populations of the three levels are c_1 , c_2 , and c_3 , then they satisfy the following equations:

$$\begin{aligned} i\dot{c}_1 &= -E_1 c_1 + \Omega_{12} c_2, \\ i\dot{c}_2 &= \Omega_{12} c_1 + \Omega_{23} c_3, \\ i\dot{c}_3 &= \Omega_{23} c_2. \end{aligned} \quad (2)$$

This set of equations can be solved for the n -photon Rabi frequency out of level 1 in the following way. First, let

$$\begin{aligned} c_+ &= \frac{c_2 + c_3}{\sqrt{2}}, \\ c_- &= \frac{c_2 - c_3}{\sqrt{2}}. \end{aligned} \quad (3)$$

With this, Eq. (2) becomes

$$\begin{aligned} i\dot{c}_1 &= -E_1 c_1 + \frac{\Omega_{12}}{\sqrt{2}} c_+ + \frac{\Omega_{12}}{\sqrt{2}} c_-, \\ i\dot{c}_+ &= \frac{\Omega_{12}}{\sqrt{2}} c_1 + \Omega_{23} c_+, \\ i\dot{c}_- &= \frac{\Omega_{12}}{\sqrt{2}} c_1 - \Omega_{23} c_-. \end{aligned} \quad (4)$$

The rapidly varying phase of each amplitude can be removed with the following transformation:

$$\begin{aligned} c_1 &= d_1 e^{iE_1 t}, \\ c_+ &= d_+ e^{-i\phi(t)}, \\ c_- &= d_- e^{i\phi(t)}, \end{aligned} \quad (5)$$

where $\phi(t) = \int_{t_0}^t \Omega_{23}(t') dt'$ and the initial conditions are specified at t_0 . The equations for the slowly varying envelopes are

$$\begin{aligned}
i\dot{d}_1 &= \frac{e^{-iE_1t}}{\sqrt{2}}(\Omega_{12}e^{-i\phi}d_+ + \Omega_{12}e^{i\phi}d_-), \\
i\dot{d}_+ &= \frac{e^{iE_1t}}{\sqrt{2}}\Omega_{12}e^{i\phi}d_1, \\
i\dot{d}_- &= \frac{e^{iE_1t}}{\sqrt{2}}\Omega_{12}e^{-i\phi}d_1.
\end{aligned} \tag{6}$$

Thus far, the manipulation of the equations has been exact. At this point, the multiphoton nature of the interaction enters through the terms $\Omega_{12}e^{\pm i\phi}$. Consider a square pulse $f(t)=1$ with field strength F_o . Then $\Omega_{12}=R_{12}F_o\sin(\omega t)$ and $\phi(t)=z\cos(\omega t)$, where $z=(R_{23}F_o/\omega)$. The term $e^{\pm iz\cos(\omega t)}$ has the well-known expansion [11],

$$e^{\pm iz\cos(\omega t)} = J_0(z) + 2\sum_{k=1}^{\infty} (\pm i)^k J_k(z)\cos(k\omega t), \tag{7}$$

where $J_n(z)$ is the Bessel function of order n . We are interested in a multiphoton resonance, where $n\omega \approx E_1$. Using the recursion relationship between the Bessel functions,

$$\frac{2\nu}{z}J_\nu(z) = J_{\nu-1}(z) + J_{\nu+1}(z), \tag{8}$$

we can find the $\pm n\omega$ components in the term $\sin(\omega t)e^{\pm iz\cos(\omega t)}$:

$$A_n = (\pm 1)^n B_n (e^{in\omega t} - e^{-in\omega t}), \tag{9}$$

where $B_n = [-i^n n/z]J_n(z)$. Returning to Eq. (6), and only keeping terms with $n\omega - E_1 = 0$, we have

$$\begin{aligned}
i\dot{d}_1 &= \frac{1}{\sqrt{2}}R_{12}F_o[B_n d_+ + (-1)^n B_n d_-], \\
i\dot{d}_+ &= \frac{1}{\sqrt{2}}R_{12}F_o B_n d_1, \\
i\dot{d}_- &= \frac{1}{\sqrt{2}}(-1)^n R_{12}F_o B_n d_1.
\end{aligned} \tag{10}$$

Finally, with one more transformation,

$$\begin{aligned}
d_2 &= \frac{d_+ + d_-}{\sqrt{2}}, \\
d_3 &= \frac{d_+ - d_-}{\sqrt{2}},
\end{aligned} \tag{11}$$

we have, for an odd value of n ,

$$i\dot{d}_1 = R_{12}F_o B_n d_+,$$

$$\begin{aligned}
i\dot{d}_2 &= R_{12}F_o B_n d_1, \\
i\dot{d}_3 &= 0,
\end{aligned} \tag{12}$$

and, for an even value of n ,

$$\begin{aligned}
i\dot{d}_1 &= R_{12}F_o B_n d_-, \\
i\dot{d}_2 &= 0, \\
i\dot{d}_3 &= R_{12}F_o B_n d_1.
\end{aligned} \tag{13}$$

Since the Rabi frequency is simply twice the magnitude of the coupling between the levels, the n -photon Rabi frequency is given by

$$\Omega_n^{(3-level)}(F_o) = 2n\omega \left(\frac{R_{12}}{R_{23}}\right) J_n\left(\frac{R_{23}F_o}{\omega}\right). \tag{14}$$

B. Discussion of the 2-level model

If the coupling between the upper levels in Fig. 1 is removed ($\Omega_{23}=0$) this system reduces to the standard 2-level model, which has been extensively studied [3,12]. The full solution to this system is rather complex, although a simple approximate expression for the n -photon Rabi frequency is given in Ref. [3]:

$$\Omega_n^{(2-level)}(F_o) = \frac{2\omega}{\pi} \left(\frac{eR_{12}F_o}{2n\omega}\right)^n, \tag{15}$$

where $e=2.7183$. Besides the Rabi frequency, Ref. [3] also gives the ac Stark shift in the 2-level system:

$$\Delta = \Omega_{12}^2/E_1. \tag{16}$$

The main difficulty with the 2-level system is that both the Rabi frequency and the ac Stark shift depend on the same coupling, Ω_{12} . Increasing the coupling to enhance the multiphoton transition rate also increases the Stark shift making it difficult to maintain the multiphoton resonance.

C. Fourier expansion of Floquet states

Perhaps the most important distinction between the 2-level and 3-level models is that in the latter case, the multiphoton coupling is generated by Ω_{23} [see Eq. (14)] while the coupling with the ground state, and hence the ac Stark shift of the ground states depends on Ω_{12} . Because of this, it is possible to have a strong multiphoton coupling with a small Stark shift if $R_{23} \gg R_{12}$. As mentioned above, this is not possible in the 2-level system as the two effects depend on the same coupling.

The consequence of these differences can be demonstrated through some simple numerical examples. First, consider the 2-level system, which is defined by letting $E_1=1.0$, $R_{12}=1$, $R_{23}=0$, $\omega=0.1$, $F_o=0.3$, and $f(t)=\exp(-t^2/\tau^2)$, where $\tau=937.5$. If we let $c_2=1$ and integrate through the pulse, we obtain the amplitudes c_1 and c_2 as a function of time. The Fourier transforms of these amplitudes

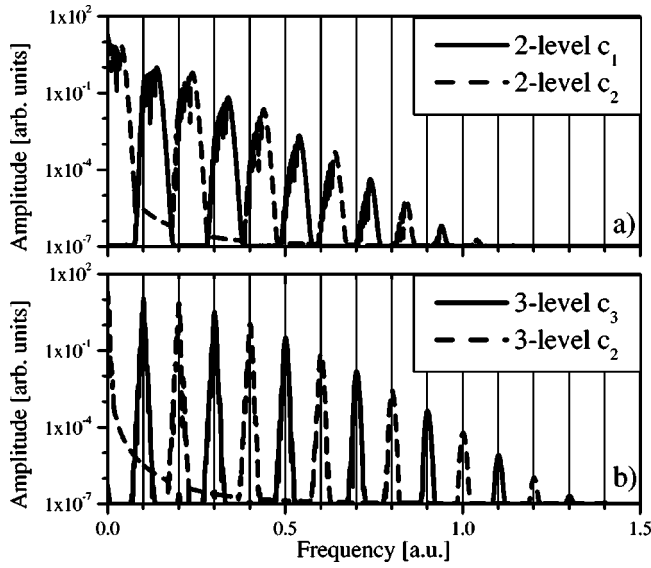


FIG. 2. The Fourier spectra of the driven population amplitudes in the (a) 2-level and (b) 3-level systems.

reveal the frequency content of the amplitudes and are shown in Fig. 2(a). First, it can be seen that there are frequency components roughly at each multiple of the photon frequency. These peaks are responsible for the multiphoton transitions. However, each peak is considerably broadened and shifted from $n\omega$. This results from the substantial time-dependent ac Stark shift.

In contrast, the upper levels of the 3-level system can be analyzed by letting $R_{12}=0.2$ and $R_{23}=1$, while keeping the other parameters the same. Here, the main coupling is now between levels 2 and 3, although a weak coupling is maintained between 1 and 2. Again we let $c_2=1$, integrate through the pulse and take the Fourier transforms of the amplitudes $c_2(t)$ and $c_3(t)$, shown in Fig. 2(b). Now the spectrum consists of sharp peaks centered almost exactly at $n\omega$, despite the fact that there is still a coupling to the ground state. There is a small shift of the peaks due to the coupling of the ground state, although it is much less than the shift in the 2-level system. Furthermore, the modulation extends to a higher order ($n=13$ as compared to $n=9$). Thus, the degenerate upper levels of the 3-level system efficiently modulate the field, creating high-frequency components without the detrimental Stark shifting of the levels.

These Fourier components essentially represent Floquet states. In the 3-level system, the driven upper states create a ladder of Floquet states that are locked to the energy of the upper states. This is because the modulation of the upper states is linear in the field and, thus, has a time average of zero [4]. This is shown schematically in Fig. 3. To produce a transition from the ground state to the upper states, there only needs to be a weak 1-photon coupling from the ground state to the lowest rung on the Floquet ladder. Although this 1-photon coupling will produce a Stark shift, the shift will be much smaller than in the 2-level system.

D. Comparison of the 2-level and 3-level models

To quantitatively demonstrate the advantages of the 3-level system, I calculated the photon frequency and field

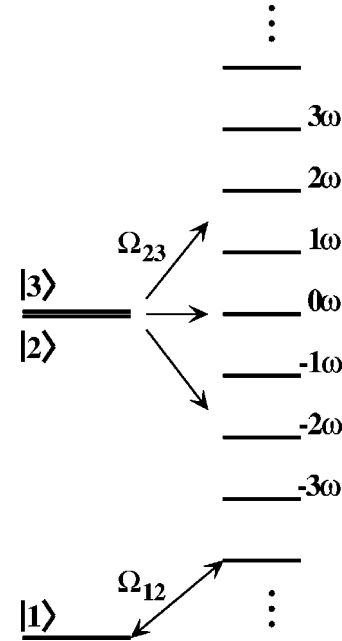


FIG. 3. Couplings in the 3-level system showing the Floquet ladder of states produced by the upper states along with the 1-photon transition to the ground state.

strength required for complete population transfer using a multiphoton transition with and without the coupling between the upper two levels for two different pulse shapes, square and Gaussian.

First, consider a square pulse of duration T . For the 2-level system, $E_1=1.0$, $R_{12}=1.0$, $R_{23}=0$, and $T=500$. For each value of n , the photon order, Eq. (2) was integrated to find the field strength F_o and frequency ω that produced a π pulse. The results are shown in Fig. 4. The results for the 3-level system are obtained in the same way, except that $R_{23}=5$. In the next section, it will be shown that this is a physically reasonable ratio between R_{12} and R_{23} . Note that

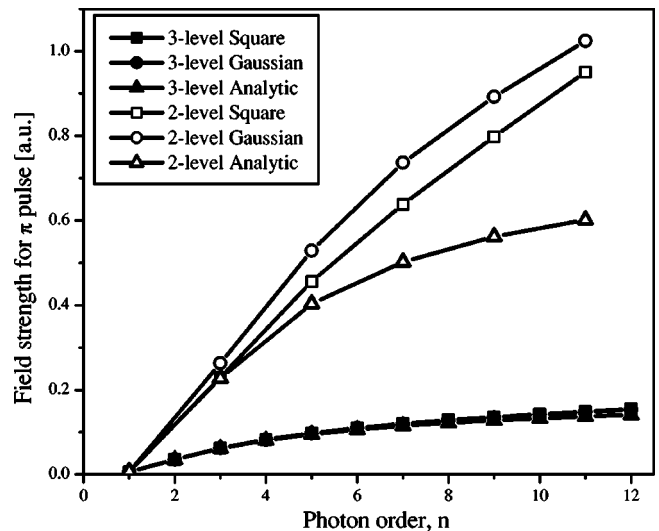


FIG. 4. Field strength F_o required for a π pulse as a function of photon order n under a variety of conditions.

the 3-level system will support even order transitions, as one upper level has even parity while the other has odd. Thus, results are given for every value of n , whereas the 2-level system only allows odd order transitions.

Also shown in Fig. 4 are the results for a Gaussian pulse shape. In order to compare the field strengths for the two different pulse shapes, it is important to conserve the ‘‘pulse area.’’ For a single-photon interaction, the pulse area is defined as

$$P_1 = \int_{-\infty}^{\infty} \Omega_1 f(t) dt, \quad (17)$$

where $\Omega_1 = RF_o$ is the 1-photon Rabi frequency. Clearly, for a square pulse of duration T , the pulse area is simply $P_1(\text{square}) = \Omega_1 T$. For a Gaussian pulse, $f(t) = \exp(-t^2/\tau^2)$, the pulse area is $P_1(\text{Gaussian}) = \Omega_1 \tau \sqrt{\pi}$. For a multiphoton interaction of order n , the Rabi frequency scales as the interaction to the n th power, $\Omega_n = (RF_o)^n$, and so the n -photon pulse area becomes

$$P_n = \int_{-\infty}^{\infty} \Omega_n f(t)^n dt. \quad (18)$$

For a square pulse, $P_n(\text{square}) = \Omega_n T$, while for a Gaussian pulse, $P_n(\text{Gaussian}) = \Omega_n \tau \sqrt{\pi/n}$. Thus, to compare a square pulse to a Gaussian pulse, all that is required is to choose $\tau = \sqrt{n/\pi} T$, as was done for Fig. 4. Finally, the analytic solutions are obtained for the square pulse shape by finding the field strength F_o such that $\Omega_n(F_o)T = \pi$, where Ω_n is given by Eq. (15) for the 2-level system and Eq. (14) for the 3-level system.

The data in Fig. 4 clearly show the large differences between the 2- and 3-level systems. First, the 2-level system requires much higher field strengths to drive a π pulse. This is not just a consequence of the stronger coupling in the 3-level system (where $R_{23} = 5R_{12}$), as for $n > 5$, the field strength is more than a factor of 5 larger for the 2-level system compared to the 3-level system. Rather, the nonlinear modulation created by the coupling between levels 2 and 3 is more efficient than that of levels 1 and 2. Moreover, as a function of n , the 2-level field strength is steady rising, while, for the 3-level system, the field appears to be saturating. Thus, the advantage of the 3-level system increases with higher order. Second, the analytic results are much better for the 3-level system than for the 2-level. The 2-level system cannot be solved exactly and a number of approximations are required to arrive at Eq. (15). In contrast, Eq. (14) is exact for the contribution of the n -photon transition and agrees very well with the numerical calculations.

Another difference between the 2- and 3-level systems is seen by comparing the results from the square and Gaussian pulse shapes. In the 2-level system, a significantly higher field strength is required for the Gaussian pulse as compared to the square pulse. This results from the large ac Stark shifts in the 2-level system.

To recover the ac Stark shift from the numerical calculations, I actually consider the total transition energy in the laser field, which is simply equal to $n\omega$, where ω is the

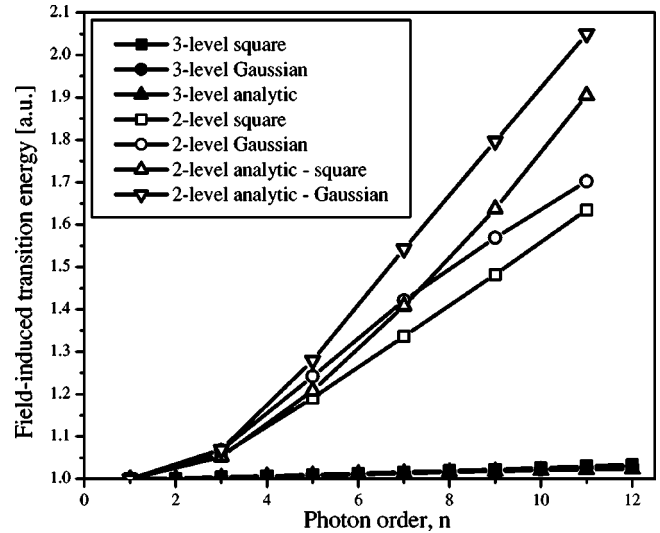


FIG. 5. Field-induced transition energy for the data in Fig. 4.

frequency needed to produce a π pulse of a given order n . Since the field-free transition energy in these examples is 1.0, the ac Stark shift Δ is now $\Delta = n\omega - 1.0$. The field-induced transition energies are shown in Fig. 5. The analytic results in all cases are simply given by the field-free transition energy plus the ac Stark shift from Eq. (16).

As can be seen in Fig. 5, there is a dramatic difference in the ac Stark shifts between the 2- and 3-level systems. Again, this is because the multiphoton coupling in the 2-level system is also responsible for the ac Stark shift, while in the 3-level system the multiphoton coupling and the ac Stark shift are distinct. As a result, in the 2-level system driven by a pulsed external field, the levels will rapidly shift in and out of resonance during the pulse, making the excitation less efficient. Thus, a higher field strength is required for the Gaussian pulse to overcome the short time that the field is in resonance, as seen in Fig. 4. The higher field strength, in turn, leads to a higher ac Stark shift, as seen in Fig. 5. In the 3-level system all of these problems are minimized, because the Stark shift is so small in the first place. Square and Gaussian pulses drive the transition equally well and the resulting Stark shifts are the same. The discrepancies in the analytic and calculated ac Stark shifts for the 2-level system in Fig. 5 simply indicate that Eq. (16) is no longer valid, as this expression is only the lowest-order term.

On the one hand, although it is always possible to find conditions in the 2-level system producing a π pulse, the results are somewhat artificial: at these high field strengths, ionization will certainly set in. On the other hand, the results for the 3-level system do open up the possibility of high-order π pulses, as the problem of the ac Stark shift has been largely removed. All of these observations of the 2-level system are in agreement with the discussion in Ref. [3].

E. The nondegenerate 3-level model

Although the above discussion demonstrates the potential of the 3-level system to provide strong multiphoton excitation, only the case of degenerate upper states has been con-

sidered. In any physical system, no two states are perfectly degenerate, and, thus, the next question is how degenerate must the upper states be to provide strong multiphoton coupling with minimal ac Stark shifts?

To proceed, it is necessary to find the Floquet energies of two nearly degenerate levels in an ac field. The results need to be exact as a function of field strength, although they can be perturbative in the splitting δ .

Consider the Hamiltonian for just the two upper states from Eq. (1):

$$H(t) = \begin{bmatrix} 0 & \Omega_{23} \\ \Omega_{23} & \delta \end{bmatrix}. \quad (19)$$

Here, we take $\Omega_{23} = R_{23}F_o \cos(\omega t)$, as it simplifies the derivation. Using the earlier notation for the upper levels of the 3-level system, amplitudes $c_2(t)$ and $c_3(t)$ satisfy

$$\begin{aligned} i\dot{c}_2 &= \Omega_{23}c_3, \\ i\dot{c}_3 &= \Omega_{23}c_2 + \delta c_3. \end{aligned} \quad (20)$$

The Floquet energies are defined by the eigenvalues of the time-development operator evolving the system through exactly one period, $T = 2\pi/\omega$, of the driving field [13]. Thus, we need to find $c_2(T)$ and $c_3(T)$ for the two sets of initial conditions: $c_2(0) = 1, c_3(0) = 0$ and $c_2(0) = 0, c_3(0) = 1$.

We proceed by making the same change of variable as in Eq. (3), giving

$$\begin{aligned} i\dot{c}_+ &= \Omega_{23}c_+ + \delta(c_+ - c_-)/2, \\ i\dot{c}_- &= -\delta(c_+ - c_-)/2 - \Omega_{23}c_-. \end{aligned} \quad (21)$$

To obtain a perturbative result, let

$$\begin{aligned} c_+ &= c_+^{(0)} + c_+^{(1)} + \dots, \\ c_- &= c_-^{(0)} + c_-^{(1)} + \dots. \end{aligned} \quad (22)$$

The zeroth order solution corresponds to neglecting the terms with δ in Eq. (21):

$$\begin{aligned} c_+^{(0)} &= e^{-i\phi(t)}c_+(0), \\ c_-^{(0)} &= e^{i\phi(t)}c_-(0), \end{aligned} \quad (23)$$

where $\phi(t) = \int_0^t \Omega_{23} dt' = (R_{23}F_o/\omega)\sin(\omega t)$. Because $\phi(T) = \phi(0)$, we have

$$\begin{aligned} c_+^{(0)}(T) &= c_+^{(0)}(0), \\ c_-^{(0)}(T) &= c_-^{(0)}(0). \end{aligned} \quad (24)$$

The first-order terms satisfy the following equations:

$$\begin{aligned} i\dot{c}_+^{(1)} &= \Omega_{23}c_+^{(1)} + (\delta/2)(c_+^{(0)} - c_-^{(0)}), \\ i\dot{c}_-^{(1)} &= -(\delta/2)(c_+^{(0)} - c_-^{(0)}) - \Omega_{23}c_-^{(1)}. \end{aligned} \quad (25)$$

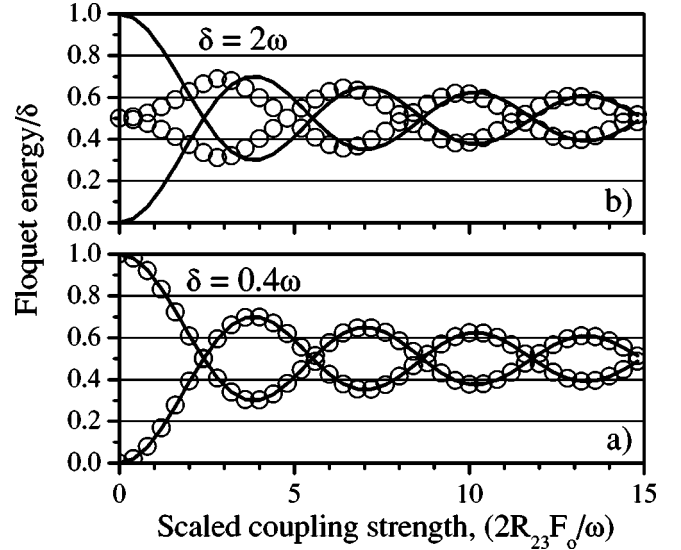


FIG. 6. The calculated Floquet eigenvalues (\circ) for two levels in an external field with frequency ω as a function of coupling strength along with the analytic expression ($-$) from Eq. (31). (a) $\delta = 0.01, \omega = 0.05$ and (b) $\delta = 0.10, \omega = 0.05$.

Making the same transformation as in Eq. (5) yields

$$\begin{aligned} i\dot{d}_+^{(1)} &= +(\delta/2)[c_+(0) - e^{2i\phi}c_-(0)], \\ i\dot{d}_-^{(1)} &= -(\delta/2)[e^{-2i\phi}c_+(0) - c_-(0)]. \end{aligned} \quad (26)$$

We are really interested in just $d_+^{(1)}(T)$ and $d_-^{(1)}(T)$, so

$$\begin{aligned} d_+^{(1)}(T) &= -i(\delta/2) \int_0^T [c_+(0) - e^{2i\phi(t')}c_-(0)] dt', \\ d_-^{(1)}(T) &= +i(\delta/2) \int_0^T [e^{-2i\phi(t')}c_+(0) - c_-(0)] dt'. \end{aligned} \quad (27)$$

Using an expression similar to Eq. (7), we have

$$\int_0^T e^{\pm 2i\phi(t')} dt' = J_0(2R_{23}F_o/\omega)T \quad (28)$$

because all of the higher-order terms in the expansion of $e^{\pm 2i\phi(t)}$ integrate to 0 over one cycle of the field. Thus,

$$\begin{aligned} d_+^{(1)}(T) &= -i(\delta T/2)[c_+(0) - J_0(2R_{23}F_o/\omega)c_-(0)], \\ d_-^{(1)}(T) &= +i(\delta T/2)[J_0(2R_{23}F_o/\omega)c_+(0) - c_-(0)]. \end{aligned} \quad (29)$$

Transforming back to c_2 and c_3 gives

$$\begin{aligned} c_2(T) &= \{1 - i(\delta T/2)[1 - J_0(2R_{23}F_o/\omega)]\}c_2(0), \\ c_3(T) &= \{1 - i(\delta T/2)(1 + J_0(2R_{23}F_o/\omega))\}c_3(0). \end{aligned} \quad (30)$$

Now, by inspection, we can see that the two eigenvalues are

$$\lambda_{\pm} = (\delta/2)[1 \pm J_0(2R_{23}F_o/\omega)]. \quad (31)$$

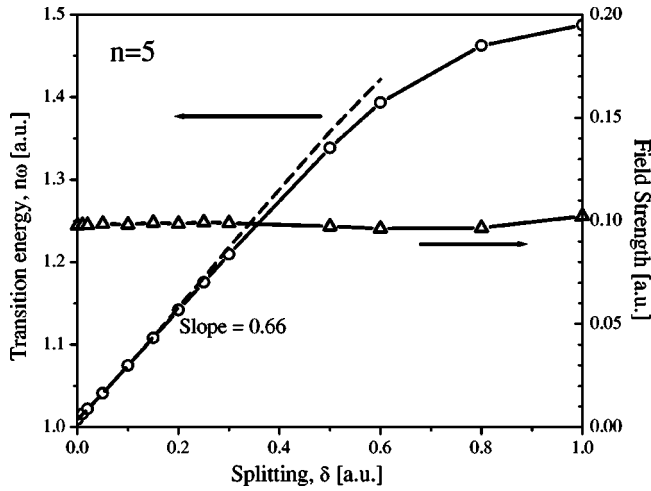


FIG. 7. Transition energy $n\omega$ (\circ) and field strength (Δ) for a π pulse as a function of splitting δ between the upper states for a 5-photon process. Also included is the analytic result for the transition energy (---). $E_1=1.0$, $R_{12}=1.0$, $R_{23}=5.0$, and $T=500$ (square pulse shape).

Figure 6 shows a comparison between the exact Floquet calculations based on numerically integrating Eq. (20) and the analytic result, Eq. (31). For $\delta < \omega$ [Fig. 6(a)], the agreement is excellent. However, even for values of δ greater than ω , Eq. (31) works surprisingly well [Fig. 6(b)]. The greatest discrepancy occurs at low coupling strength but the analytic results converge to the exact values, as the coupling strength is increased.

These results show that the energies of levels 2 and 3 will change as a function of the field strength and this is potentially a problem for the 3-level system, just as the ac Stark shift of the ground state is a problem for the 2-level system. Two regimes need to be considered. For relatively large values of ω , the scaled coupling strength $z=2R_{23}F_o/\omega$ is not so large and is on the order of 4 for the example of $n=5$ in Fig. 4. In this case, the Floquet energy is not changing rapidly at the strongest part of the pulse, and will simply shift in energy by about 0.7δ . This contrasts with the normal ac Stark shift, which always changes rapidly as a function of the field strength. For small values of ω (or a high-order multiphoton resonance) the scaled coupling z will be much larger, on the order of 14 for $n=12$ in Fig. 4. In this case, the Floquet energy is constantly changing as a function of field strength, but it oscillates around $\delta/2$ and the total excursion is roughly $\delta/4$. There is already an ac Stark shift of the ground state given by Eq. (16); so as long as the shift of the Floquet energy is on this order, it should not affect the interaction significantly, i.e., for

$$\delta < 4\Omega_{12}^2/E_1. \quad (32)$$

In fact, for an even-order transition, the down shift of level 3 could be used to compensate the ac Stark shift of the ground state.

To investigate the effects of the splitting on the conditions necessary for creating π pulses, Figs. 7 and 8 show the results of numerical calculations similar to those in the last

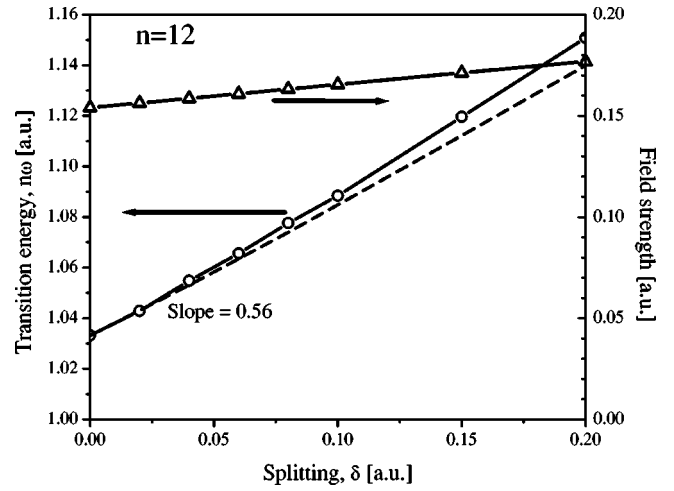


FIG. 8. Transition energy $n\omega$ (\circ) and field strength (Δ) for a π pulse as a function of splitting δ between the upper states for a 12-photon process. Also included is the analytic result for the transition energy (---). $E_1=1.0$, $R_{12}=1.0$, $R_{23}=5.0$, and $T=500$ (square pulse shape).

section. As before, the matrix elements are $R_{12}=1.0$ and $R_{23}=5.0$, and a square pulse with a duration of $T=500$ is used. $E_1=1.0$ and the energy of level 2 is zero, as before, but now, level 3 is placed at a positive value of δ . The transition energy E_T is defined as before.

Figure 7 shows results for a 5-photon transition. Because this is an odd number of photons the transition will be between levels 1 and 2. Over a large range of δ , E_T is linear in δ . The slope of 0.66 is very close to the maximum value of 0.7 discussed above. The analytic result from Eq. (31) agrees well with the data, especially for small splitting. Most importantly, the required field strength is essentially independent of δ . Figure 8 shows similar results for a 12-photon transition. All other parameters are the same as in Fig. 7. In this case, the scaled coupling strength is on the order of $z=18$ where the transition energy would be expected to follow 0.5δ , and this is indeed close to what is seen. Again, the analytic result agrees fairly well with the calculations. Interestingly, the agreement between the analytic values and the calculations persists significantly into the region where $\delta > \omega$, as might be expected from the results in Fig. 6. At field strengths where significant multiphoton excitation takes place, it turns out that Eq. (31) is valid even when the splitting is greater than the laser frequency. However, it should be noted that these calculations were based on the conditions for completely depopulating the ground state. When $\delta \approx \omega$, the population will end up in a mixture of the upper states.

F. Conclusions

In this section, I have presented a 3-level system that has a very strong multiphoton coupling between a far off-resonant ground state and a pair of strongly coupled upper states. The strong coupling of the upper states effectively modulates the field to make multiphoton transitions with the ground state possible. Essentially, this creates a ladder of the Floquet states. The ground state needs only couple to the

closest Floquet state in a 1-photon transition that only requires a weak coupling. As a result, the ac Stark shift of the ground state is extremely small. Moreover, the requirement that the upper states be nearly degenerate is actually not very stringent. Splittings up to twice the photon energy have little impact on the field strength needed for the multiphoton transition. Although the upper levels shift in energy, they shift in a predictable way that can be taken into account. Nevertheless, this 3-level system provides a robust way to drive very high order multiphoton transitions to the point where π pulses appear to be attainable.

What remains to be shown is that these results apply in conditions where ionization is present. This can be done by considering a full quantum mechanical system with energy levels and couplings corresponding to the 3-level system, but that also contains ionization. This is done in the following section.

III. MODEL MOLECULAR SYSTEM: A_2^{4+}

A. Motivation

Although the 3-level system analyzed in Sec. II clearly shows that high-order multiphoton processes can be driven much more efficiently than in the 2-level system, it is not obvious that the 3-level system will work well in a real setting. Real systems, of course, have other levels present, which can interact with the levels of the 3-level structure. These interactions can lead to large ac Stark shifts that were not accounted for in the analysis of the 3-level system. Also, the extra levels can divert population from the target level. Although these extra levels need to be considered, ionization is probably the more serious problem. In the original discussion of 2-level systems, it was the fact that ionization will compete with excitation that ultimately led to the conclusion that multiphoton excitation will never be effective [3].

Before considering possible effects that can interfere with the 3-level system, we must first find a real system with the 3-level structure embedded in it. As mentioned above, there has been little evidence for the direct multiphoton population transfer to excited states in atoms. Multiphoton resonances play an important role in understanding the photoelectron spectrum created by strong field ionization—the so-called “Freeman resonance” [14]. Here, the Rydberg states of an atom are shifted in energy by the ponderomotive potential, which is proportional to the laser intensity. As the states are shifted during the pulse, they will pass through multiphoton resonances with the ground state. At these points, the ionization rate increases significantly leading to a characteristic Rydberg-type structure in the electron spectrum. This type of multiphoton excitation illustrates the problems with a 2-level interaction: the amount of excitation per level is very small, and the population is easily ionized. Thus, atoms do not appear to be promising candidates for efficient multiphoton excitation.

Unlike atoms, diatomic molecules have consistently shown evidence for reasonably strong multiphoton excitation in one specific instance: the simple observation of the charge asymmetric dissociation of diatomic molecules ionized by strong laser fields [6,8,9,15]. For example, the nitrogen mol-

ecule can easily be ionized up to N_2^{4+} by a short pulse laser. This molecular ion will then immediately dissociate into $N^{2+} + N^{2+}$. This charge-symmetric dissociation (CSD) is the ground-state channel. However, it has also been observed that the original molecular ion can dissociate into $N^{3+} + N^{1+}$, the charge-asymmetric dissociation (CAD) channel. The potential energy curves corresponding to the CAD channel lie significantly higher in energy (≈ 18 eV) than the curves leading to CSD. This means that the original N_2^{4+} molecule must be in a highly excited state for it to be able to access the CAD channel [15].

The process that populates the excited states leading to CAD must be quite general and robust, as CAD is seen in at least N_2 , O_2 , and I_2 . In iodine, the efficiency of the excitation (defined by the ratio of the CAD channel to the sum of the CAD and CSD channels) is in the range of 10–30% for ultrashort (~ 30 fs) laser pulses [9]. Moreover, CAD has been observed up to $I_2^{12+} \rightarrow I^{7+} + I^{5+}$ [9]. Thus, evenly charged homonuclear diatomic molecules must have a generic structure that make them quite susceptible to strong field excitation. In the following section, I will show what is unique about the structure of these molecules.

B. Ionic states and molecular orbitals

The simplest model of an evenly charged homonuclear diatomic molecule consists of two electrons in a double-well potential with an internuclear separation D . To get a sense of the energy level structure, let $|\alpha\rangle$ and $|\beta\rangle$ be the ground-state 1-electron wave functions in the left and right wells, respectively. From these orbitals, we can form the symmetric (singlet) covalent ground state:

$$\Psi_{ground}^g = \frac{|\alpha\rangle|\beta\rangle + |\beta\rangle|\alpha\rangle}{\sqrt{2}}. \quad (33)$$

There will also be two symmetric excited states with ionic character:

$$\begin{aligned} \Psi_{ionic}^g &= \frac{|\alpha\rangle|\alpha\rangle + |\beta\rangle|\beta\rangle}{\sqrt{2}}, \\ \Psi_{ionic}^u &= \frac{|\alpha\rangle|\alpha\rangle - |\beta\rangle|\beta\rangle}{\sqrt{2}}. \end{aligned} \quad (34)$$

The g and u superscripts refer to gerade and ungerade symmetry, respectively. There is no antisymmetric (triplet) equivalent to these ionic states, so I will only consider the singlet states in this model.

Often, these states are written in the following form, based on the molecular orbitals, $1\sigma_g = (|\alpha\rangle + |\beta\rangle)/\sqrt{2}$ and $1\sigma_u = (|\alpha\rangle - |\beta\rangle)/\sqrt{2}$ [5]:

$$\begin{aligned} \Psi_{ground}^g &= (|\alpha\rangle + |\beta\rangle)(|\alpha\rangle + |\beta\rangle)/2, \\ \Psi_{ionic}^g &= (|\alpha\rangle - |\beta\rangle)(|\alpha\rangle - |\beta\rangle)/2, \\ \Psi_{ionic}^u &= (|\alpha\rangle + |\beta\rangle)(|\alpha\rangle - |\beta\rangle)/2. \end{aligned} \quad (35)$$

However, there is a strong configuration interaction between the Ψ_{ground}^g and Ψ_{ionic}^g states in Eq. (35) and they do not have the correct asymptotic form for large D . Whether Eqs. (33) and (34) or Eq. (35) are the correct basis depends on both the charge state of the molecule and the internuclear separation. For high charge states and large D , the former is more accurate, while for a neutral molecule at its equilibrium separation, the latter is better. In the following section, I will be considering the case of a four-times ionized molecule where the former description applies.

As we will see in the following numerical calculations, Ψ_{ionic}^g and Ψ_{ionic}^u are nearly degenerate and have a dipole coupling that approaches D , as D gets large, while the coupling between Ψ_{ground}^g and Ψ_{ionic}^u is relatively weak. Furthermore, there is a large energy gap between Ψ_{ground}^g and the ionic pair. Thus, these three states have energy levels and dipole couplings corresponding to the 3-level system analyzed above. Moreover, this structure also corresponds to the experimental observations discussed above: the covalent ground state will dissociate into the charge-symmetric fragments, while the ionic states will dissociate into the charge-asymmetric fragments. The importance of the pair of ionic states in strong field dynamics has recently been discussed in Refs. [16,17].

C. 1D molecular model

The molecular system discussed in the preceding section can be modeled by a 1D Hamiltonian consisting of a spatial term H_s and a momentum term H_p : $H(t) = H_s(t) + H_p(t)$, where $H_p(p_1, p_2, t) = p_1^2/2 + p_2^2/2$ and

$$H_s(x_1, x_2, t) = \frac{-Z}{\sqrt{(x_1-d)^2 + a^2}} + \frac{-Z}{\sqrt{(x_1+d)^2 + a^2}} + \frac{-Z}{\sqrt{(x_2-d)^2 + a^2}} + \frac{-Z}{\sqrt{(x_2+d)^2 + a^2}} + \frac{1}{\sqrt{(x_1-x_2)^2 + a^2}} + (x_1+x_2)F(t). \quad (36)$$

$D=2d$ is the internuclear separation, $F(t)$ is the electric field strength, a is a smoothing parameter, Z is the charge on each atom, and x_1, x_2 (p_1, p_2) are the positions (momenta) of the electrons. This 1D ‘‘soft Coulomb’’ potential has been widely used to study strong field interactions with both 2-electron atoms [18] and molecules [16]. All wave functions are stored on a 135×135 spatial grid with a step size of 0.15. An absorbing boundary is placed around the edge of the grid to account for ionization. Although this is a rather small area, we are only interested in the bound part of the wave function and not the dynamics of the ionized electrons. Several checks were performed with a larger grid and/or smaller step size and no significant differences were found.

To propagate the wave function through one time step, the spatial part of the Hamiltonian is first applied as $\exp(-iH_s\Delta t)$, where $\Delta t=0.1$. The wave function is then transformed into momentum space through a fast complex

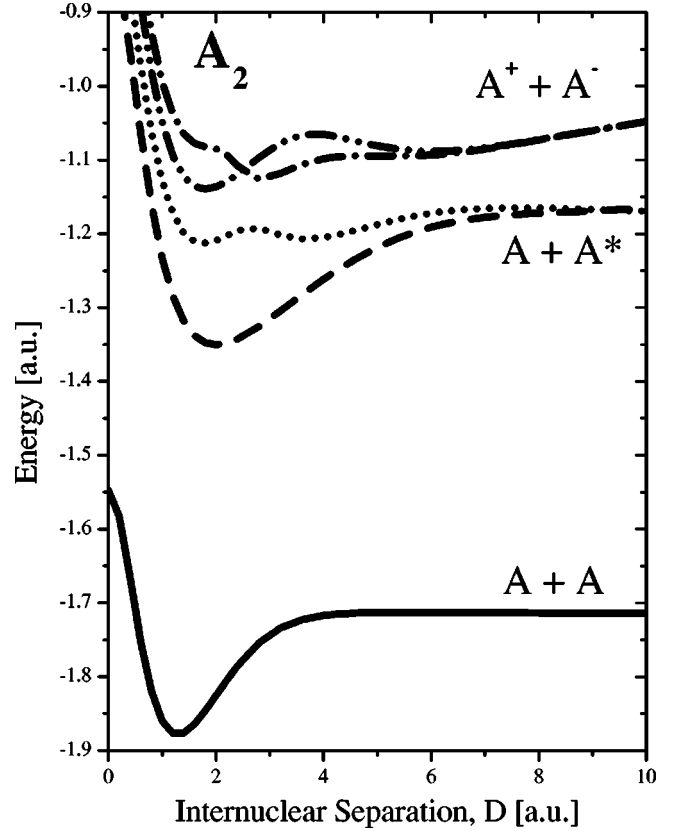


FIG. 9. Potential energy curves for the model molecule A_2 ($Z=1$), including the internuclear repulsion, Z^2/D .

Fourier transform, where the momentum Hamiltonian $\exp(-iH_p\Delta t)$ is applied. Finally, the wave function is transformed back to real space. As mentioned in the preceding section, several checks were performed to determine the effect of the choice of the interaction, Fx vs Ap , on the results. In all cases, the final populations differed by less than 1%.

Before each calculation the wave functions of the lowest five states are found by assigning random numbers to the grid and integrating the system in imaginary time. In this way, all states decay exponentially with a time constant equal to the energy of the state. However, the wave function is renormalized on each time step. Since the ground state will have the longest decay time, the initial wave function will evolve into the ground state.

The excited states are found by the same way, except that before renormalizing the wave function on each step, the ground state and all previously found excited states are projected out. In this way, the lowest energy state that has not already been found will be produced. During the projection and renormalization, the symmetry of the wave function is also imposed. As discussed above, symmetric wave functions are used throughout.

Figure 9 shows the five lowest energy levels of this Hamiltonian as a function of internuclear separation D for $Z=1$ and $a=0.742$, which roughly corresponds to N_2 , while Fig. 10 shows the results for $Z=3$, corresponding to N_2^{4+} .

In Fig. 9, as is well known, the ionic curves cross the excited state covalent curves, leading to strong mixing. As a

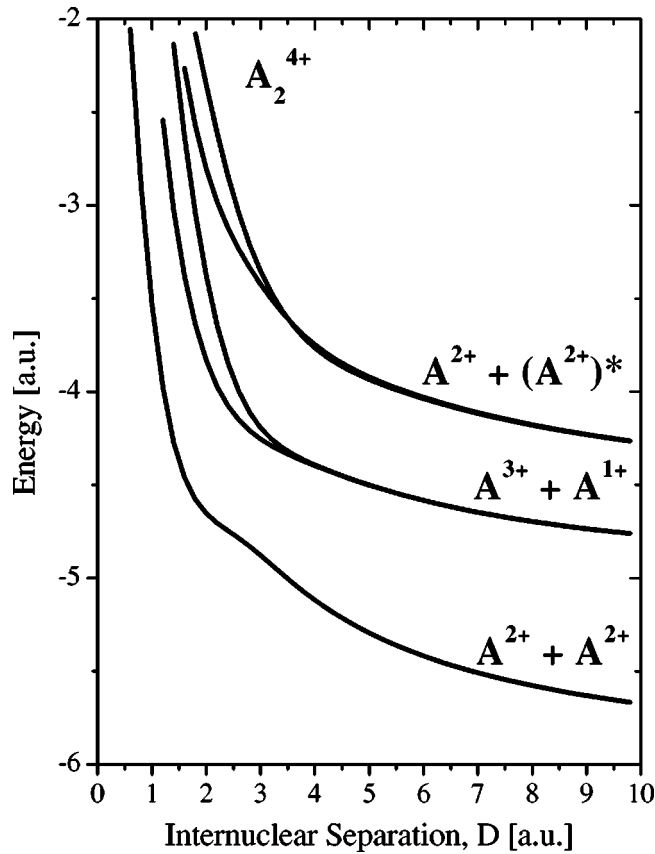


FIG. 10. Potential energy curves for the model molecule A_2^{4+} ($Z=3$), including the internuclear repulsion, Z^2/D .

result, at any value of D , it is hard to classify the states based on ionic or covalent character. In the highly ionized molecule, the situation is rather different. The excited covalent curves lie above the ionic ones, and the states retain their character. In the following, we will restrict our attention to the highly ionized molecule.

As can be seen in Fig. 10, there is a large energy gap between the ground and first excited states. Moreover, the first excited states are actually a pair of nearly degenerate states with opposite parity and hence are strongly coupled. The gerade ionic state actually lies slightly higher in energy than the ungerade state, probably due to the configuration interaction with the gerade ground state. Thus, the correspondence between these states and the levels in the 3-level system are the following: level 1 \leftrightarrow ground state, level 2 \leftrightarrow ionic ungerade state, and level 3 \leftrightarrow ionic gerade state.

With the wave functions determined, we can also plot the dipole coupling between the states as a function of D , as well as the splitting of the ionic states (Fig. 11). The latter is important for making the connection to the 3-level system. As can be seen in Fig. 11, R_{23} asymptotically approaches D . Also, for $D > 2$, R_{12} drops exponentially, and so the limit $R_{23} \gg R_{12}$ is quickly reached for increasing D . The splitting δ drops to zero even faster. Thus, for the values of $D \geq 3$, this molecular system has all the important characteristics of the 3-level system.

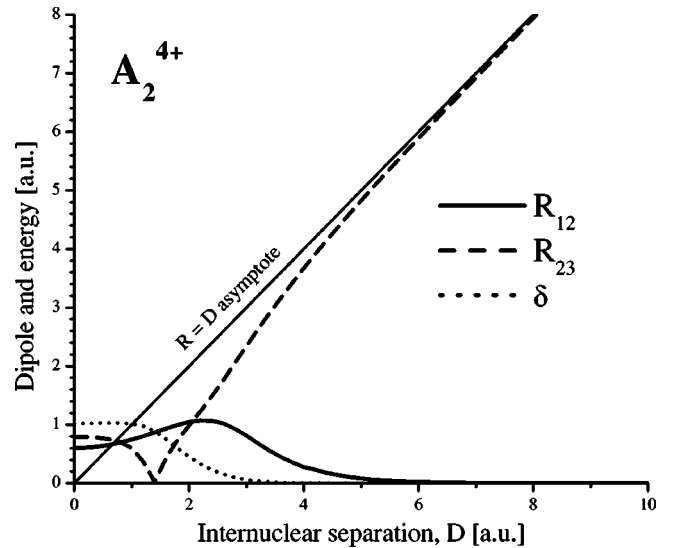


FIG. 11. Dipole coupling between the ground and ungerade ionic states (R_{12}) and between the ionic states (R_{23}) in the model molecule A_2^{4+} , as well as the splitting δ of the ionic states.

D. Numerical results for population transfer

The A_2^{4+} model molecule is a complicated system. My intention is not to fully analyze all of its possible responses to a strong laser field, but simply to show that π pulses can be driven to either of the ionic states without ionization. To make a comparison between the analytic results for the 3-level system and the molecular model, let us consider, for example, a 12-photon transition between the ground state and the ionic gerade state (levels 1 and 3) at an internuclear separation of $D=3.5$. At this point, the energies of the first three levels in the model are -5.0038 , -4.3353 , -4.3186 . In the 3-level notation, this gives $E_1=0.6685$ and $\delta=0.0167$. For a 12-photon resonance, the laser frequency is $\omega=(E_1+\delta)/12=0.0571$. The coupling strengths are $R_{12}=0.503$ and $R_{23}=3.033$.

In the calculations a Gaussian pulse with a full width at half maximum in intensity of 244 a.u. was used. With this, we can use Eq. (14) to find the field strength required for a π pulse, which gives $F_o=0.2095$. At this field strength the ac Stark shift of the ground state is, from Eq. (16), -0.0162 . The coupling of levels 2 and 3 is in the strong field limit, giving a downward shift of level 3 approximately equal to $\delta/2=0.00835$. These shifts partially cancel, leading to a field-induced transition energy $E_T=0.6931$ and $\omega=0.0578$ for a 12-photon resonance. It is important to note that, if the same coupling strength were present between levels 1 and 2 as between levels 2 and 3, the ac Stark shift of the ground state would be -0.6069 . Thus, the small shifts from the ac Stark shift and splitting between the upper states are much smaller than the ac Stark shift that would have been present in a similar 2-level system. Figure 12 shows the results of the calculation for these parameters at a field strength of $F_o=0.21$. The populations of the three lowest levels are plotted as a function of laser frequency, ω .

Several important features are seen in Fig. 12. First, very efficient population transfer can be produced on a 12-photon

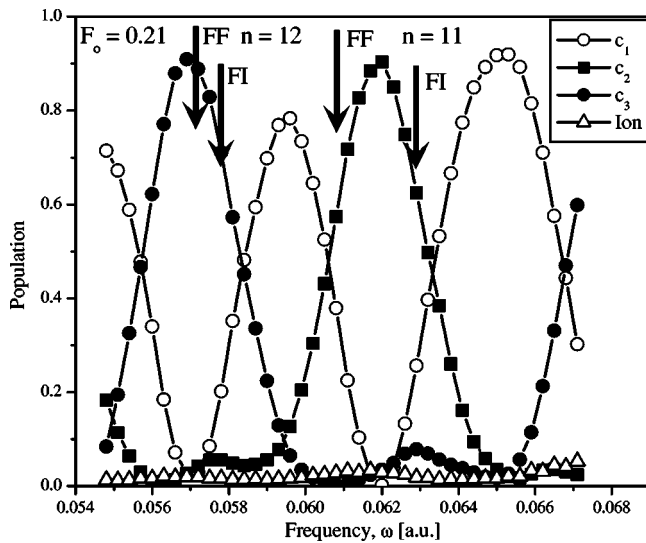


FIG. 12. Final population of the three lowest states of A_2^{4+} , as well as the ionized fraction as a function of laser frequency ω , for a pulse duration of 244 a.u.; $D=3.5$. Also marked are the predicted field-free (FF) and field-induced (FI) transition frequencies for both the $n=11$ and $n=12$ resonances.

resonance in a real quantum mechanical system. Over 90% of the population can be driven into the excited state with almost no ionization. The field strength predicted from Eq. (14) turns out to be very accurate. The exact position of the resonance turns out to be slightly different than the predicted value, although it is almost exactly equal to the field-free value. Thus, both ionization and the influence of other states are very small in this molecular model. The $n=11$ multiphoton transition to the ungerade ionic state also appears in Fig. 12. Similar conclusions hold for this transition: over 90% population transfer occurs, while the ground state is completely depopulated with little ionization.

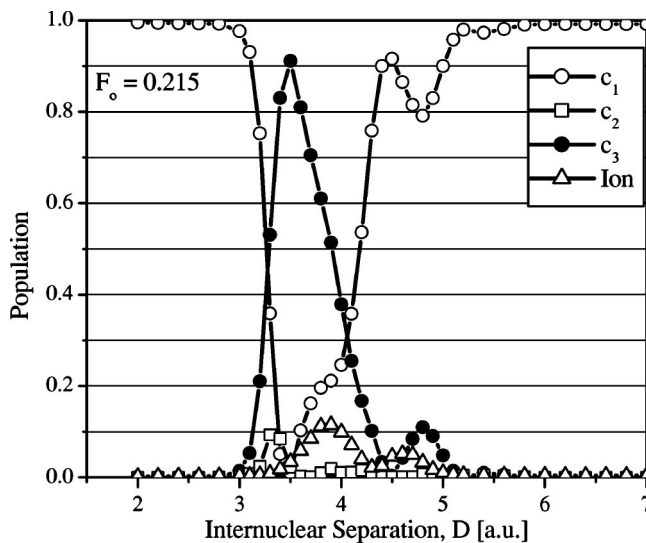


FIG. 13. Final population of the three lowest states of A_2^{4+} as well as ionization as a function of internuclear separation for a pulse duration of 244 a.u.; $\omega=0.0570$.

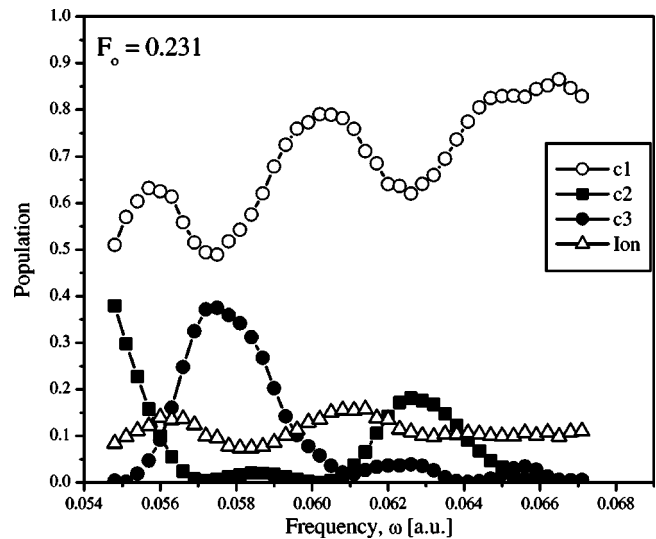


FIG. 14. Final population of the three lowest states of A_2^{4+} as well as the ionized fraction as a function of laser frequency ω , for a pulse duration of 244 a.u.; $D=3.5$.

Another scenario involves holding the field strength and laser frequency constant and varying the internuclear separation. The reason for this is that in a real experiment, the laser frequency is more easily held constant, while the molecule dissociates. Thus, the molecule automatically scans the internuclear separation and will find a multiphoton resonance at some point. This is shown in Fig. 13. The maximum excitation occurs at $D=3.5$, right at the point where the field-free levels come into a 12-photon resonance with the laser field. Again, a near complete inversion is obtained with little ionization.

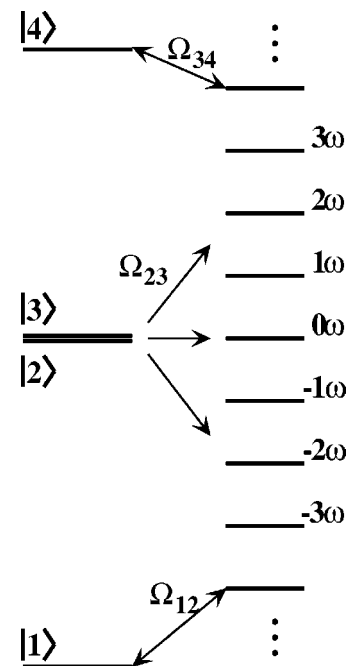


FIG. 15. Energy levels in a more complex system showing that the Floquet ladder could connect the ground state to very highly excited states through Ω_{34} .

At higher field strengths, the π pulse is overdriven and other effects come into play, as seen in Fig. 14. At this point, ionization starts to become more prominent and the final population in level 3 is significantly lower. Also, at a frequency of $\omega=0.56$, for example, 4% of the population is unaccounted for by the three lowest levels and ionization. Thus, some population is getting into more highly excited states. Thus, although we can see the effects of ionization and other levels in the system, these effects are quite small and the interaction is dominated by the 3-level structure at the intensities where π pulses can be driven.

A real system, such as N_2^{4+} will be yet more complex than the 2-electron calculations. Here again, the reduced field strength and the ac Stark shift is highly advantageous. Extraneous states are less likely to couple to the ground state, as they will generally be nonresonant and will produce less of a Stark shift of the upper states. However, additional states do raise a different possibility—the strongly coupled pair of levels can be the lower levels of a 3-level system as well. Once the molecule has been excited from the ground state to the pair of excited states, as the molecule continues to dissociate, this pair may come into resonance with an even higher state, Fig. 15. At this point, there will be a strong coupling (Ω_{34}) with this state, further exciting the molecule. This may ex-

plain the observation that the fragment ions following charge-asymmetric dissociation can themselves be in an excited state [19].

IV. CONCLUSIONS

In conclusion, I have presented a 3-level system that allows for strong multiphoton excitation of high-lying states. This level structure occurs naturally in even-charged diatomic molecules and can explain why evidence for excitation by strong laser fields has been so conspicuous in molecules while almost completely absent in atoms. The pair of nearly degenerate strongly coupled levels acts as a very efficient modulator without producing detrimental Stark shifts. Odd-charged molecules, such as N_2^{3+} , also have pairs of strongly coupled states and may also provide a suitable system for this kind of multiphoton excitation.

ACKNOWLEDGMENTS

I would like to acknowledge useful conversations with G. Dunne, R. Jones, and J. Javanainen, as well as support from the NSF under Grant No. NSF-PHYS-9987804.

-
- [1] C.K. Rhodes, *Science* **229**, 1345 (1985).
 - [2] C.W. Clark, M.G. Littman, R.B. Miles, T.J. McIlrath, C.H. Skinner, S. Suckewer, and E. Valeo, *J. Opt. Soc. Am. B* **3**, 371 (1986).
 - [3] R.E. Duvall, E.J. Valeo, and C.R. Oberman, *Phys. Rev. A* **37**, 4685 (1988).
 - [4] G.N. Gibson, *Phys. Rev. Lett.* **89**, 263001 (2002).
 - [5] R.S. Mulliken, *J. Chem. Phys.* **7**, 20 (1939).
 - [6] K. Boyer, T.S. Luk, J.C. Solem, and C.K. Rhodes, *Phys. Rev. A* **39**, 1186 (1989).
 - [7] G. Gibson, T.S. Luk, A. McPherson, K. Boyer, and C.K. Rhodes, *Phys. Rev. A* **40**, 2378 (1989).
 - [8] D.T. Strickland, Y. Beaudoin, P. Dietrich, and P.B. Corkum, *Phys. Rev. Lett.* **68**, 2755 (1992).
 - [9] G.N. Gibson, M. Li, C. Guo, and J.P. Nibarger, *Phys. Rev. A* **58**, 4723 (1998).
 - [10] F. Bassani, J.J. Forney, and A. Quattropani, *Phys. Rev. Lett.* **39**, 1070 (1977).
 - [11] M. Abramowitz and I. Stegun, *Handbook of Mathematical Functions* (Dover, New York, 1998).
 - [12] J.H. Shirley, *Phys. Rev.* **138**, B979 (1965).
 - [13] I. Tittonen, M. Lippmaa, and J. Javanainen, *Phys. Rev. A* **53**, 1112 (1996).
 - [14] R.R. Freeman and P.H. Bucksbaum, *J. Phys. B* **24**, 3325 (1991).
 - [15] J.P. Nibarger, S.V. Menon, and G.N. Gibson, *Phys. Rev. A* **63**, 053406 (2001).
 - [16] I. Kawata, H. Kono, Y. Fujimura, and A.D. Bandrauk, *Phys. Rev. A* **62**, 031401(R) (2000).
 - [17] S.V. Menon, J.P. Nibarger, and G.N. Gibson, *J. Phys. B* **35**, 2961 (2002).
 - [18] W.-C. Liu, J.H. Eberly, S.L. Haan, and R. Grobe, *Phys. Rev. Lett.* **83**, 520 (1999).
 - [19] J.P. Nibarger, M. Li, S. Menon, and G.N. Gibson, *Phys. Rev. Lett.* **83**, 4975 (1999).